



EPA Public Access

Author manuscript

J Mol Catal A Chem. Author manuscript; available in PMC 2018 September 19.

About author manuscripts

Submit a manuscript

Published in final edited form as:

J Mol Catal A Chem. 2016 December 15; 425(0): 183–189. doi:10.1016/j.molcata.2016.09.035.

Use of Selected Scavengers for the Determination of NF-TiO₂ Reactive Oxygen Species during the Degradation of Microcystin-LR under Visible Light Irradiation

MIGUEL PELAEZ¹, POLYCARPOS FALARAS², VLASSIS LIKODIMOS², KEVIN O'SHEA³, ARMAH A. de la CRUZ⁴, PATRICK S.M. DUNLOP⁵, J. ANTHONY BYRNE⁵, and DIONYSIOS D. DIONYSIOU^{*,1}

¹Environmental Engineering and Science Program, University of Cincinnati, Cincinnati, Ohio 45221-0071, USA

²Institute of Physical Chemistry, NCSR Demokritos, 15310 Aghia Paraskevi Attikis, Athens, Greece

³Department of Chemistry and Biochemistry, Florida International University, University Park, Miami, Florida 3319, USA

⁴Office of Research and Development, U.S. Environmental Protection Agency, Cincinnati, OH 45268, USA

⁵Nanotechnology and Integrated BioEngineering Centre, School of Engineering, University of Ulster, Northern Ireland, BT37 0QB, United Kingdom

Abstract

Although UV-induced TiO₂ photocatalysis involves the generation of several reactive oxygen species (ROS), the formation of hydroxyl radicals are generally associated with the degradation of persistent organic contaminants in water. In this study, a variety of radical scavengers were employed to discriminate the roles of different ROS during visible light activated (VLA) photocatalysis using nitrogen and fluorine doped TiO₂ (NF-TiO₂) in the degradation of the hepatotoxin, microcystin-LR (MC-LR) in water. The addition of hydroxyl radical scavengers, methanol and *tert*-butyl alcohol to the reaction mixture resulted in negligible inhibition of VLA NF-TiO₂ photocatalytic degradation of MCLR at pH 3.0 and only partial inhibition at pH 5.7. While hydroxyl radicals generally play the primary role in UV TiO₂ photocatalysis, the minimal influence of MeOH and *t*-BuOH on the degradation process under these experimental conditions indicates hydroxyl radicals ([•]OH) do not play the primary role in VLA NF-TiO₂ photocatalysis. However, strong inhibition was observed in VLA NF-TiO₂ photocatalytic degradation of MC-LR in the presence of superoxide dismutase, benzoquinone and catalase at pH 3.0 and 5.7 indicating O₂^{•-} and H₂O₂ play critical roles in the degradation process. Similar degradation rates were observed in the presence of singlet oxygen scavenger, deuterium oxide, which enhances singlet oxygen mediated processes further suggesting singlet oxygen does not play a key role in the

*Corresponding author phone: (513) 556-0724; fax: (513) 556-2599; dionysios.d.dionysiou@uc.edu.

Disclaimer: The research described in this article has not been subjected to the Agency's required peer and policy review and therefore does not necessarily reflect the views of the Agency and no official endorsement should be inferred.

degradation of MCLR in these system. Formic acid and cupric nitrate were added to probe the roles of the valence band holes and conduction band electrons, respectively. Under UV+vis light irradiation, almost complete inhibition of MC-LR removal is observed with NF-TiO₂ in the presence of •OH scavengers at pH 5.7. These results demonstrate that solution pH plays a major role in the formation and reactivities of ROS during VLA NF-TiO₂ photocatalysis. The adsorption strength of the scavengers and MCLR onto NF-TiO₂ as well as the speciation of the ROS as a function of pH need to be carefully considered since they also play a key role in the efficiency of the process. These results indicate the reduction of molecular oxygen by photo-generated electrons rather than hydroxyl radicals produced by oxidative reactions of photo-generated holes play a key role in the of VLA NF-TiO₂ photocatalytic degradation of MC-LR.

Keywords

NF-TiO₂; photocatalysis; scavenger; reactive oxygen species; hydroxyl radical; superoxide radical anion; singlet oxygen; visible light; microcystin-LR; water treatment

1. Introduction

The primary electronic processes in TiO₂ photocatalysis under UV light involves the absorption of a photon with energy equal or greater to its band gap (3.2 eV for anatase and brookite TiO₂ and 3.0 eV for rutile TiO₂) that excites an electron to the conduction band (e^-_{CB}) generating a hole in the valence band (h^+_{VB}) [1-4]. These charge carriers can migrate to the catalyst surface and initiate redox reactions where the h^+_{VB} can oxidize OH⁻ or water adsorbed at the surface to produce reactive oxygen species (ROS), mainly hydroxyl radicals (•OH), while e^-_{CB} can be scavenged by adsorbed molecular oxygen leading to the formation of superoxide radical anions (O₂^{•-}). O₂^{•-} may further react to form singlet oxygen and hydrogen peroxide where the latter can produce •OH as well [1]. Interfacial charge transfer from the photogenerated electron/holes to acceptor/donor species at the surface competes with charge recombination at surface trapping sites or in the bulk of TiO₂. Recombination of the electron/hole pair results in loss of adsorbed photonic energy with release of heat by non-radiative decay processes. The generation of ROS by TiO₂ photocatalysis for upon illumination by UV light along with its environmentally benign properties (i.e. non-toxicity, absence of dissolution in water, photostability) and relatively low cost, render TiO₂ photocatalysis a critical option for the remediation of recalcitrant organic pollutants in water and air as well as for killing pathogenic microorganisms [2-4]. Despite the marked progress in TiO₂ photocatalytic materials, their practical application is challenged by two inherent limitations of TiO₂: 1) the low quantum yield i.e., the ratio of reactant molecules destroyed or the product molecules formed during the photocatalytic reaction to the quantity of absorbed photons at a given wavelength [1], which is primarily determined by the recombination of photogenerated charge carriers, and 2) the relatively poor solar light harvesting that is limited by the wide band gap of TiO₂ in the UVA spectral range. Both factors undermine the photocatalytic efficiency of TiO₂ and its enormous potential as an essential “green” technology for the destruction of noxious organic compounds in water and air under solar light. The modification and further development of TiO₂-based photocatalytic technology towards visible light activation will provide an opportunity to develop a

nanocatalysts that can absorb both UV (290-400 nm) and visible (400-700 nm) radiation to enhance the overall process efficiency and employ solar light as a renewable source of energy. Visible light activation of TiO₂ has been intensively pursued recently by diverse approaches including photosensitization with dyes, modification with metal and non-metal atoms and coupling with narrow band gap semiconductors [5-8, 9]. Nevertheless, the photocatalytic degradation mechanisms associated with VLA TiO₂ photocatalysis are still ambiguous and the formation and role of different ROS are unclear.

In dye-sensitized TiO₂ photocatalysis, the dye absorbs visible light instead of TiO₂ and becomes photo-excited [6]. The electrons from the excited dye molecule are subsequently transferred into the conduction band of TiO₂ and react with molecular oxygen to produce ROS. Recent work by Diaz-Urbe *et al.*, suggests the formation of O₂^{•-} with tetra(4-carboxyphenyl)porphyrin sensitized TiO₂ but no singlet oxygen was detected using electron paramagnetic resonance (EPR); even though the possibility was not excluded completely [10]. Goldstein *et al.*, concluded that oxidation of methanol was governed by the generation of surface holes followed by organic radical-based attack in carbon doped TiO₂ photocatalysis under VLA [11]. Based on EPR studies using spin traps, Fu *et al.*, provided evidence that •OH and O₂^{•-} were responsible for the photodegradation of 4-CP by VLA activated nitrogen-doped TiO₂ (N-TiO₂) nanoparticles [12]. For nitrogen and sulfur doped TiO₂ nanoparticles, EPR spin trapping studies suggest, O₂^{•-} and singlet oxygen were formed upon visible light illumination and were responsible of the inactivation of *Escherichia coli* in water [13]. A chemiluminescence technique quantified an increase of singlet oxygen production when using a composite TiO₂/N-TiO₂ photocatalyst under visible light irradiation for NO_x decomposition compared to N-TiO₂ only. As for TiO₂, the characteristic 1268 nm emission of singlet oxygen was not detected upon visible light irradiation [14]. Recent developments and insights in this field highlight the need to further develop and understand the mechanisms of these photocatalyst for environmental remediation [15].

Therefore, the main objective of this study was to elucidate the formation of ROS with a visible light-activated TiO₂ photocatalyst using selected chemical probe scavengers that are specific for •OH, O₂^{•-}, singlet oxygen and the photogenerated electron-hole pairs. NF-TiO₂ have been successfully synthesized, characterized and evaluated for its photocatalytic activity under visible light [16, 17]. The use of scavengers will contribute to a better basic understanding of the photocatalytic mechanism of NF-TiO₂ towards the degradation of the cyanobacterial toxin microcystin-LR (MC-LR). MC-LR is a highly toxic, commonly found and highly persistent cyanotoxin released or secreted from cyanobacterial harmful algae blooms in surface water [18, 19]. The presence of these toxins in recreational water bodies and drinking water sources are a serious concern to the environmental and health authorities because of the significant health risk to humans and the environment.

2. Materials and methods

2.1 Chemicals and NF-TiO₂ synthesis

Methanol (MeOH, Tedia) and *tert*-butyl alcohol (TBA, Fisher) were used as hydroxyl radical scavengers. Deuterium oxide (D₂O, Acros Organics) was used as singlet oxygen scavenger. For the inhibition of superoxide radical anion, 1,4-benzoquinone (98%, Sigma Aldrich) and

superoxide dismutase (SOD, Sigma Aldrich) from *Escherichia coli* (manganese-containing enzyme, lyophilized, activity 1,000 units/mg protein). The electron and hole pair was scavenged with cupric nitrate (Fisher) and formic acid (88% Fisher), respectively. The nitrate salt of Cu^{2+} was used since adsorption of the nitrate anions onto TiO_2 's surface is weak. Catalase from bovine liver was obtained from Sigma Aldrich and used as H_2O_2 inhibitor. L-histidine (98%, Acros Organics) was used during UV illumination to scavenge singlet oxygen and hydroxyl radicals. Nitric acid was used to adjust the pH at 3.0 in experiments dealing with acidic pH. Finally, MC-LR standard (dry solid, 500 μg) was obtained from Calbiochem. The nanotechnological approach for the synthesis of NF- TiO_2 consisted in the use of a nonionic fluorosurfactant as pore template and fluorine dopant and ethylenediamine as nitrogen dopant as described in detail in [16]. The resulting nanoparticles exhibited high BET surface area (141 m^2/g), high porosity (49%), small crystallite size (8.7 nm) and with a nitrogen and fluorine content of 1.5% and 4.9%, respectively [16].

2.2. Scavenger experiments

A borosilicate petri dish was used as reactor and MilliQ-grade water was adjusted to the desired pH and a specific scavenger was added into solution to obtain an initial concentration of 5000 μM except for SOD and catalase where 2 μM and 10 μM were employed (see Table 1 for selected scavengers). Then the solution was spiked with an aliquot of MC-LR standard to reach an initial concentration of $500 \pm 10 \mu\text{g L}^{-1}$ which is equivalent to $0.5 \pm 0.1 \mu\text{M}$. Separately, an aqueous NF- TiO_2 suspension was prepared, sonicated and transferred to the reactor to achieve an initial concentration of 0.5 g L^{-1} and a final volume of 10 mLs. The reactor was sealed with parafilm and mixed continuously during the photocatalytic reaction with visible light irradiation. To obtain visible light irradiation only, a UV block filter (UV420, Opticology) was mounted below two 15 W fluorescent lamps (Cole-Parmer) to eliminate photons below 420 nm. Samples were taken at specific periods of time and the samples were quenched with methanol, filtered (L815, Whatman) to remove the suspended nanoparticles, transferred to 0.2 ml glass inserts and placed in sample vials. MC-LR samples were analyzed by liquid chromatography (LC, Agilent Series 1100). The analytical conditions were similar to those reported by Antoniou *et al.*, [19] but the column employed was a C_{18} Discovery (Supelco) column (150 \times 2.1 mm, 5.0 μm particle size). The flow rate was 0.2 ml/min, the injection volume was 20 μl and the column temperature was 40 $^\circ\text{C}$.

3. Results and Discussion

3.1. $\cdot\text{OH}$ scavengers

To probe the role of hydroxyl radical in the photocatalytic degradation of MC-LR by VLA NF- TiO_2 , a number of experiments were conducted in the absence and presence of methanol or TBA at pH 3.0 and 5.7 (see Figure 1a and 1b). Methanol and TBA react rapidly with hydroxyl radical and have been used extensively as $\cdot\text{OH}$ scavengers to determine the presence and role of hydroxyl radicals in TiO_2 photocatalysis under UV light. The addition of methanol and TBA dramatically reduces the degradation rate of the targeted contaminants by conventional UV TiO_2 photocatalysis indicating that $\cdot\text{OH}$ mediated oxidation processes

are the predominant pathways leading to degradation under UV irradiation [20]. The solution pH influence the overall charge on the catalyst surface increases and the speciation of the ionizable functional groups present in MC-LR. The charge on the surface and specific functional group can lead to repulsive or attractive interaction between MC-LR and the catalyst surface. Under modestly acidic conditions the catalyst surface will be positive while the carboxylate group will be negative down to approximately pH 4 and thus a strong electrostatic attraction is expected to enhanced adsorption of MC-LR in this pH range. The hydrophobic character of MC-LR also increases with solution acidity, which may also contribute to increased adsorption and degradation under acidic conditions. The addition of 5000 μM of methanol or TBA did not lead to significant inhibition of the degradation of MC-LR by VLA NF-TiO₂ photocatalysis at pH 3.0, as illustrated in Figure 1a. The absence of inhibition in the presence of these scavengers suggest the minimal role of $\cdot\text{OH}$ in the degradation of MCLR under these experimental conditions. At higher pH, 5.7, partial inhibition was observed for the degradation of MC-LR in the presence of methanol and TBA. The adsorption of MC-LR onto the photocatalyst decreased as pH increased from 3.0 to 5.7 [17]. As mentioned before, MC-LR is quite hydrophobic at pH 3.0 which can enhance strong adsorption while methanol and TBA may not compete with the ROS formed. With increasing pH the adsorption of MeOH and t-BuOH may also increase leading to lower adsorption levels for MCLR effectively reducing it degradation and thus methanol or TBA can adsorb to a higher extent on the surface of NF-TiO₂. Given the high relative concentrations of scavengers and decreased adsorption of MC-LR with increasing pH these conditions may lead to the blocking of the photocatalytically active sites of NF-TiO₂ and/or partial suppression of the formation of the ROS, resulting in slower MC-LR degradation. The pka of superoxide radical anion is 4.6, which lies between 3.0 and 5.7 and this can have a pronounced effect of the subsequent chemistry of the radical. For instance, negatively charged superoxide radical anion may remain at positive surface and thus inhibit disproportionation while facilitating other pathways with singlet oxygen production.

It is well known that when conventional TiO₂ is subject to UV light illumination, the primary formation route of $\cdot\text{OH}$ is based on the oxidation of OH⁻ or water at the TiO₂ surface through the highly oxidizing and delocalized h^+_{VB} that migrated to the catalyst surface [1,3,4]. Also, the formation of H₂O₂ (that occurs upon the reduction of molecular oxygen acting as an electron acceptor) can also generate $\cdot\text{OH}$ via homolytic scission in a secondary reaction pathway [1] although it is highly influenced by pH. In the case of non-metal doped TiO₂, in particular nitrogen-doped TiO₂, it has been proposed that the introduction of single N hetero-atoms in the TiO₂ lattice (substitutional or interstitial) induces localized electronic states within the titania band gap and selectively promotes electrons from these states to the conduction band upon visible light irradiation [21]. Under this condition, the photogenerated holes in the localized intra-gap energy states may not have a positive enough electrochemical reduction potential to generate hydroxyl radicals at the surface of the catalyst from oxidation of absorbed water or hydroxyl groups. However, the formation of $\cdot\text{OH}$ radicals through the reaction of photoinduced e^- and/or O₂^{•-} with H₂O₂ (H₂O + H⁺ + e⁻_{CB} → $\cdot\text{OH}$ + H₂O; H₂O₂ + O₂^{•-} → $\cdot\text{OH}$ + OH⁻ + O₂) as secondary reaction pathways should not be discarded (see section 3.2 for O₂^{•-} and H₂O₂ formation). Under visible light irradiation, the direct photolysis of H₂O₂ to produce $\cdot\text{OH}$ can be

neglected due to the small molar absorption coefficient ($< 1 \text{ M}^{-1} \text{ cm}^{-1}$ above 300 nm) [22]. Nevertheless, the formation of $\cdot\text{OH}$ from H_2O_2 (with e^-_{CB}) is expected to be appreciably slower than that through surface holes at least under UV excitation according to the corresponding reduction potentials ($\text{H}_2\text{O}_2/\cdot\text{OH}$ is about 0.87 V (vs NHE) [23] and $\text{H}_2\text{O}/\cdot\text{OH}$ is about 2.27 V (vs NHE) [13] at pH 7.0 because of the multiple steps and competing pathways required to produce $\text{HO}\cdot$ from $\text{O}_2^{\cdot-}$.

Wang *et al.*, [20] reported the degradation rate of methyl orange by the visible light photocatalysis using nitrogen-doped titania nanobelts was not inhibited in the presence of methanol. The authors suggest that, the generation of electrons and $\text{O}_2^{\cdot-}$ was the rate limiting step for visible light N-doped TiO_2 photocatalysis. Mrowetz *et al.*, [24] showed that N-doped TiO_2 photocatalysis under visible light irradiation unlike UV-mediated TiO_2 photocatalysis is not capable of oxidizing HCOO^- . The lack of formic acid oxidation suggest free or adsorbed $\cdot\text{OH}$ radicals are not produced under the experimental conditions tested. While water splitting with carbon doped TiO_2 under visible light has been reported the results are subject to controversy based on photo electrochemical studies [25].

The second order rate constant of TBA and methanol with $\cdot\text{OH}$ has been reported to be 4.8×10^8 and $8.3 \times 10^8 \text{ M}^{-1} \text{ s}^{-1}$, respectively [26]. Literature values for the second order rate constant for MC-LR and $\cdot\text{OH}$ range from $1.0\text{-}2.3 (\pm 0.1) \times 10^{10} \text{ M}^{-1} \text{ s}^{-1}$ [27]. If hydroxyl radicals were the primary species leading to the degradation of MC-LR during VLA NF- TiO_2 photocatalysis, addition of TBA or methanol should inhibit the degradation. The minimal level of inhibition observed upon addition of hydroxyl radical indicates the hydroxyl-radical-based oxidation pathway does not play a significant role in the degradation of MC-LR with NF- TiO_2 under visible light irradiation (at the conditions tested) although the $\cdot\text{OH}$ formation can undergo multistep process through reduction of molecular oxygen to $\text{O}_2^{\cdot-}$, disproportionation to H_2O_2 and subsequent reduction to $\cdot\text{OH}$.

3.2. $\text{O}_2^{\cdot-}$ scavengers

SOD and 1,4-benzoquinone were used as scavengers to probe the formation and role of $\text{O}_2^{\cdot-}$ during VLA NF- TiO_2 photocatalysis. The inhibition of MC-LR degradation increases with increasing SOD from 2 to 10 μM at pH 3.0, illustrated in Figure 2a. Significant inhibition of MC-LR was also observed in the presence of 1,4-benzoquinone. These results suggest that $\text{O}_2^{\cdot-}$ is an important oxidant in the VLA NF- TiO_2 photocatalysis. The inhibition of the MC-LR photocatalytic degradation was more pronounced with the addition of SOD and catalase. SOD catalyzes the conversion of $\text{O}_2^{\cdot-}$ into H_2O_2 and oxygen, while catalase converts H_2O_2 to water and oxygen. H_2O_2 is produced by SOD, which can lead to the formation of $\cdot\text{OH}$ (see section 3.1) in the absence of catalase although this could be a very low yield pathway. At pH 5.7, complete inhibition was observed with 1,4-benzoquinone according to Figure 2b. Higher inhibition with SOD and catalase was also observed at pH 5.7 compared to pH 3.0. The pKa of 1,4-benzoquinone is 9.9 and 11.4 [28] so at both pH values the interaction with NF- TiO_2 was low. The isoelectric point of SOD occurs at pH 5.0 [29] thus in solution above pH 5.0, SOD has an overall negative charge, which may enhance interaction with the positively charged surface of NF- TiO_2 at pH 5.7. In addition, the pKa for superoxide is 4.6

thus at pH below 4.6 the neutral form is dominant (HO_2^\bullet) and above pH 4.6 the anionic form ($\text{O}_2^{\bullet-}$) is dominant.

The reduction potential of conduction band electrons in NF-TiO₂ is considered equivalent to that of undoped TiO₂ [13, 30] and capable of reducing molecular oxygen at the surface of the catalyst to $\text{O}_2^{\bullet-}$ under visible light irradiation. The superoxide radical anion can act as oxidizing species for the degradation of MC-LR since the electrochemical oxidation potential (EOP) of $\text{O}_2^{\bullet-}$ is 0.57 ± 0.01 V [31]. The initial degradation of MC-LR was slower under visible light compared to UV or solar light, which is consistent with the fact that VLA yields primarily $\text{O}_2^{\bullet-}$ with an EOP = 0.57 V compared to $\bullet\text{OH}$ produced under UV and solar excitation with an EOP = 2.8 V. Further reduction of $\text{O}_2^{\bullet-}$ with e^-_{CB} can produce H_2O_2 or $\text{O}_2^{\bullet-}$ that could be further oxidized to form singlet oxygen. The production of $\text{O}_2^{\bullet-}$ has been detected using EPR during VLA N-TiO₂ photocatalysis [21]. According to recent EPR analysis [32], NF-TiO₂ comprises similar paramagnetic N centers to those of N-TiO₂ [21], with concentrations increasing dramatically upon visible light illumination, verifying the formation of localized intra-gap states above the valence band of TiO₂. These results indicate the conduction band electrons localized at N-centers in photo-excited NF-TiO₂ can yield $\text{O}_2^{\bullet-}$ via electron transfer to surface adsorbed O₂.

3.3. $^1\text{O}_2$ scavengers

To further explore the role of singlet oxygen in VLA NF-TiO₂ photocatalysis and eliminate the problems with competitive adsorption of scavengers, experiments were conducted with deuterium oxide (D_2O) as the solvent. Singlet oxygen reactions are dramatically accelerated in D_2O compared to H_2O because the lifetime of singlet oxygen is 55 μsec compared to 4.2 μsec in H_2O [33]. The photocatalytic degradation of MC-LR was slightly higher in D_2O compared to H_2O buffered at pH 7.4 as illustrated in Figure 3. Similar degradation of MC-LR was observed with buffered H_2O and buffered D_2O (pH 7.4) indicating minimal interaction of NF-TiO₂ with the ions from the buffered solution. At pH 7.4, electrostatic repulsion between negatively charged MC-LR and negatively charged NF-TiO₂ is expected to reduce the MC-LR adsorption but still ~30% degradation was observed. This indicates that reactive oxygen species are formed under D_2O as well but the results provide no direct indication on the presence of singlet oxygen. The formation of singlet oxygen is associated with the transformation of superoxide anion radicals. The redox potential of 0.34 V vs NHE indicates that the relation ($\text{O}_2^{\bullet-}/^1\text{O}_2$) is favored thermodynamically [13], but the formation of singlet oxygen is limited to the back electron transfer of an electron in $\text{O}_2^{\bullet-}$ to valence band holes. However, photogenerated holes are expected to remain localized in intra-gap energy states after charge separation in N-TiO₂ [21], which would limit the interaction with $\text{O}_2^{\bullet-}$ and the probability for the formation of singlet oxygen.

3.4 e^- and h^+ scavengers

In order to determine the involvement of e^-_{CB} and h^+ in NF-TiO₂ photocatalysis under visible light, cupric nitrate and formic acid were used as e^-_{CB} and h^+ scavengers, respectively. Rengaraj and Li employed formic acid as a hole scavenger to enhance the photocatalytic reduction reaction of Bi^{3+} -doped TiO₂ under UV light [34]. It can also inhibit the process by reacting with hydroxyl radicals and by compete adsorption with MC-LR at

the surface where ROS are produced. The inhibition of MC-LR in the presence of each scavenger is shown in Figure 4a and 4b and compared to control at pH 3.0 and 5.7. Under both pH values, partial inhibition of MC-LR degradation was observed. For the case of Cu^{2+} , the adsorption of the transition metal onto NF-TiO₂ decreased the reduction of oxygen by the conduction electrons and partially inhibited the formation of ROS and the removal of MC-LR. Chen et al., observed a hindering effect of Cu^{2+} ions on the photodegradation of three dyes using TiO₂ dispersions under visible light irradiation. The formation of ROS were blocked, based on electron spin resonance analysis, indicating that the adsorbed ions can alter the electron-transfer pathway and suppress the degradation of the dye [35]. Moreover, it is known that Cu^{2+} can be reduced by superoxide radical anion [36]. The competition for superoxide radical anions between Cu^{2+} and MC-LR can lead to a reduction in the oxidation of the cyanotoxin. The addition of formic acid at pH 3.0 and buffered pH 5.7 is anticipated to prolong the lifetime of electrons and consequently produce more $\text{O}_2^{\bullet-}$, however inhibition of the photo-oxidation process was observed. VLA NF-TiO₂ photocatalysis does not generate a valence band hole that can lead to the formation of $\bullet\text{OH}$. Therefore, the partial inhibition may result from the competition for adsorption between MC-LR and formic acid (pK_a of 3.7) since formic acid can also interact with $\bullet\text{OH}$ with a rate constant k_{HA} of $1.3 \times 10^8 \text{ M}^{-1} \text{ s}^{-1}$ and k_{A^-} of $3.2 \times 10^9 \text{ M}^{-1} \text{ s}^{-1}$ [37] but high degradation of MC-LR was still observed indicating a lack of interaction with any potentially available $\bullet\text{OH}$.

Scheme 1 shows a proposed mechanism of NF-TiO₂ photoactivation under visible light. From the findings obtained in this investigation, the mechanism of ROS formation of the synthesized photocatalyst under visible light is inferred to proceed via the reduction of molecular oxygen by visible light-excited electrons leading to the generation of superoxide radical anions and the intermediates formed and not via the generation of hydroxyl radicals by h^+ in the localized N-centers of NF-TiO₂. Superoxide is critical to the degradation process through disproportionation to H₂O₂ and the formation of HO \bullet . The production of HO \bullet under VLA is relative slow and in low yield, but localized at surface where adsorbates (such as MC-LR) are degraded. Adsorption strength plays a key role in the efficiency of the process.

3.5 $\bullet\text{OH}$ formation under UV+vis light

Figure 5 shows the photocatalytic degradation of MC-LR under UV+vis light in the absence and presence of methanol and L-histidine. Significantly faster removal of MC-LR was obtained with NF-TiO₂ only under UV+vis compared to visible light at pH 5.7. In this case, the UV+vis light source included UV radiation with high intensity peaks at 310 and 365 nm [15]. The photoactivation of NF-TiO₂ with UV light contributed to the enhanced performance of the photocatalyst towards the degradation of MC-LR. The possible generation of $\bullet\text{OH}$ under UV+vis light with NF-TiO₂ could be the responsible of this enhancement. In this case, high inhibition with methanol and L-histidine was observed at pH 5.7. L-histidine is known to be a quencher for both $^1\text{O}_2$ and $\bullet\text{OH}$ with a pK_a of 6.04 [38]. The second order rate constant of L-histidine with $\bullet\text{OH}$ is 5.0×10^9 . Contrary to the results obtained under visible light, high inhibition of MC-LR was obtained in the presence of both scavengers. This indicates the generation of hydroxyl radicals as the primary reactive oxygen species with NF-TiO₂ under UV+vis light.

4. Conclusions

In this study, the mechanism of NF-TiO₂ radical formation under visible light with selected scavengers for the degradation of MC-LR in water was systematically investigated. No direct indication for the presence of holes and [•]OH in NF-TiO₂ was obtained with formic acid and methanol, respectively, under visible light at pH 3.0 and 5.7. The formation of O₂^{•-} and H₂O₂ with NF-TiO₂ was established from the high inhibition of MC-LR degradation with superoxide dismutase and catalase at both pH values. Singlet oxygen formation is conditioned to further oxidation of O₂^{•-} with delocalized holes, whose formation could be limited in NF-TiO₂. When employing UV+vis light, it was found that [•]OH is the primary ROS formed with NF-TiO₂ due to the high inhibition on the degradation of MC-LR with methanol and L-histidine, two [•]OH scavengers, at pH 5.7. Overall, pH plays a major role in the ROS formation during NF-TiO₂ photocatalysis under visible light for the degradation of MC-LR. The affinity of the scavenger with NF-TiO₂ and MC-LR as well as the disproportionation of the ROS needs to be considered. Nevertheless, the mechanism of radical formation with NF-TiO₂ under visible light indicates that the ROS generated proceed via the oxygen reduction pathway rather than the oxidative reactions of photogenerated holes that can produce hydroxyl radicals. This study provides essential information for understanding and improving the detailed reaction mechanism underlying the photocatalytic activity of NF-TiO₂ under visible and solar light towards the degradation of cyanotoxins and other contaminants of emerging concern in water.

Acknowledgments

This work was funded by a NSF Collaborative Research (US-Ireland) (Number CBET-1033317) and the European Commission (Clean Water - Grant Agreement number 227017). Clean Water is a Collaborative Project co-funded by the Research DG of the European Commission within the joint RTD activities of the Environment and NMP Thematic Priorities/FP7.

References

1. Hoffmann MR, Martin ST, Choi W, Bahnemann DW. *Chem Rev.* 1995; 95:69–96.
2. Turchi S, Ollis DF. *J Catal.* 1990; 122:178–192.
3. Bhatkhande S, Pangarkar VG, Beenacker A. *J of Chem Technol Biotechnol.* 2001; 77:102–116.
4. Fujishima, Rao TN, Tryk DA. *J Photochem Photobiol, C.* 2000; 1:1–21.
5. Asahi R, Morikawa T, Aoki K, Taga Y. *Science.* 2001; 293:269–271. [PubMed: 11452117]
6. Kumar SG, Devi LG. *J Phys Chem A.* 2011; 115(46):13211–41. [PubMed: 21919459]
7. Li XZ, Li FB. *Environ Sci Technol.* 2001; 35:2381–2387. [PubMed: 11414049]
8. Ghows N, Entezari MH. *Ultrason Sonochem.* 2011; 18:629–634. [PubMed: 20801705]
9. Pelaez M, Nolan NT, Pillai SC, Seery MK, Falaras P, Kontos AG, Dunlop PSM, Hamilton JWJ, Byrne JA, O'Shea K, Entezari MH, Dionysiou DD. *Appl Catal B: Environmental.* 2012; 125:331–349.
10. Diaz-Uribe CE, Daza MC, Martínez F, Páez-Mozo EA, Guedes CLB, Di Mauro E. *Journal of Photochem & Photobiol A.* 2010; 215:172–178.
11. Goldstein S, Behar D, Rabani J. *J Phys Chem C.* 2008; 112:15134–15139.
12. Fu H, Zhang L, Zhang S, Zhu Y. *J Phys Chem B.* 2006; 110:3061–3065. [PubMed: 16494309]
13. Rengifo-Herrera JA, Pierzchala K, Sienkiewicz A, Forro L, Kiwi J, Pulgarin C. *Appl Catal, B.* 2009; 88:398–406.

14. Kang IC, Zhang Q, Yin S, Sato T, Saito F. *Environ Sci Technol*. 2008; 42(10):3622–3626. [PubMed: 18546699]
15. Banerjee S, Pillai SC, Falaras P, O'Shea KE, Byrne JA, Dionysiou DD. *J Phys Chem Lett*. 2014; 5:2543–2554. [PubMed: 26277942]
16. Pelaez M, de la Cruz AA, Stathatos E, Falaras P, Dionysiou DD. *Catalysis Today*. 2009; 144:19–25.
17. Pelaez M, de la Cruz AA, O'shea K, Falaras P, Dionysiou DD. *Water Research*. 2011; 45:3787–3796. [PubMed: 21575981]
18. de la Cruz AA, Antoniou MG, Hiskia A, Pelaez M, Song W, O'Shea KE, He X, Dionysiou DD. *Anti-Cancer Agents in Medicinal Chemistry*. 2011; 11:19–37. [PubMed: 21269255]
19. Antoniou MG, Shoemaker JA, de la Cruz AA, Dionysiou DD. *Toxicol*. 2008; 51:1103–1118. [PubMed: 18377943]
20. Wang J, Tafen DN, Lewis JP, Hong Z, Manivannan A, Zhi M, Li M, Wu N. *J Am Chem Soc*. 2009; 131:12290–12297. [PubMed: 19705915]
21. Livraghi S, Paganini MC, Giamello E, Selloni A, Di Valentin C, Pacchioni G. *J Am Chem Soc*. 2006; 128:15666–15671. [PubMed: 17147376]
22. Kim S, Park H, Choi W. *J Phys Chem B*. 2004; 108:6402–6411. [PubMed: 18950128]
23. Hirakawa T, Nosaka Y. *Langmuir*. 2002; 18:3247–3254.
24. Mrowetz M, Balcerski W, Colussi AJ, Hoffmann MR. *J Phys Chem B*. 2004; 108(45):17269–17273.
25. Murphy AB. *Solar Energy Materials & Solar Cells*. 2008; 92:363–367.
26. Motohashi N, Saito Y. *Chem Pharm Bull*. 1993; 41:1842–1845.
27. Song W, Xu T, Cooper WJ, Dionysiou DD, de la Cruz AA, O'Shea KE. *Environ Sci Technol*. 2009; 43(5):1487–1492. [PubMed: 19350924]
28. Nivinskas H, Staskeviciene S, Sarlauskas J, Koder RL, Miller A-F, Cenas N. *Archives of Biochemistry and Biophysics*. 2002; 403:249–258. [PubMed: 12139974]
29. Banci L, Bertini I, Turano P. *Eur Biophys J*. 1991; 19:141–146. [PubMed: 2060493]
30. Hirakawa T, Nosaka Y. *J Phys Chem C*. 2008; 112:15818–15823.
31. Rao PS, Hayon E. *Biochem Biophys Res Commun*. 1973; 51(2):468–473. [PubMed: 4693487]
32. Pelaez M, Falaras P, Likodimos V, Kontos AG, de la Cruz AA, O'Shea K, Dionysiou DD. *Appl Catal, B*. 2010; 99:378–387.
33. Rodgers MAJ. Activated oxygen. In: Bensasson RV, Jori G, Land EJ, Truscott TG, editors *Primary Photo-Processes in Biology and Medicine*. Vol. 85. 1984. 181–195. NATO ASI Series A, Life Sciences
34. Rengaraj S, Li XZ. *Chemosphere*. 2007; 66(5):930–938. [PubMed: 16859732]
35. Chen C, Li X, Ma W, Zhao J, Hidaka H, Serpone N. *J Phys Chem B*. 2002; 106(2):318–324.
36. Benzi Gianni. *Peroxidation, Energy Transduction and Mitochondria during Aging*. John Libbey Eurotext FR; 1990. The modulating and toxic significance of endocellular peroxidations; 56
37. Leitner NKV, Dore M. *Journal of Photochem & Photobiol A*. 1996; 99:137–143.
38. Ahmed A, Yao P-C, Brant AM, Peter GJ, Harper AA. *J Biol Chem*. 1997; 272(1):125–130. [PubMed: 8995237]

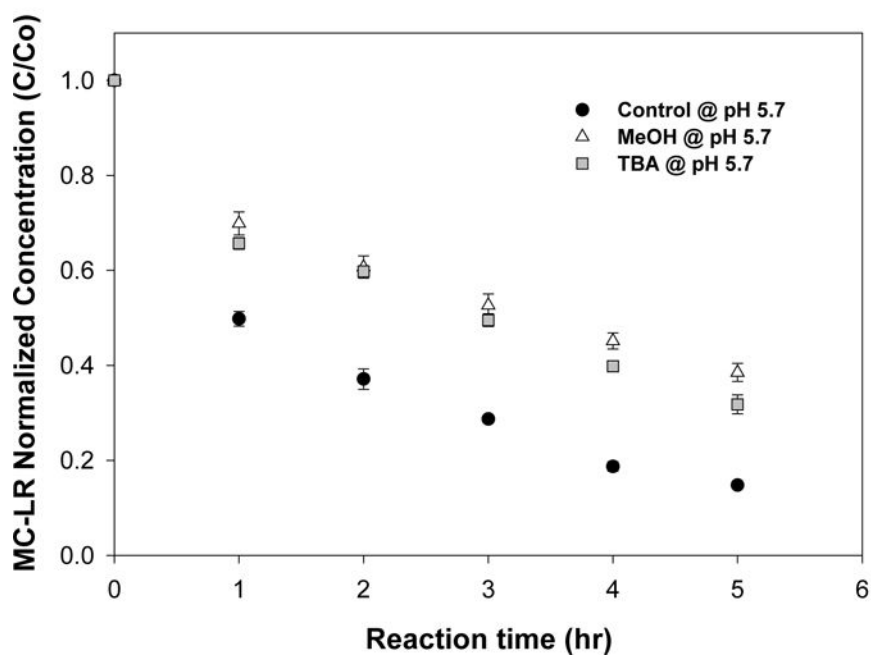
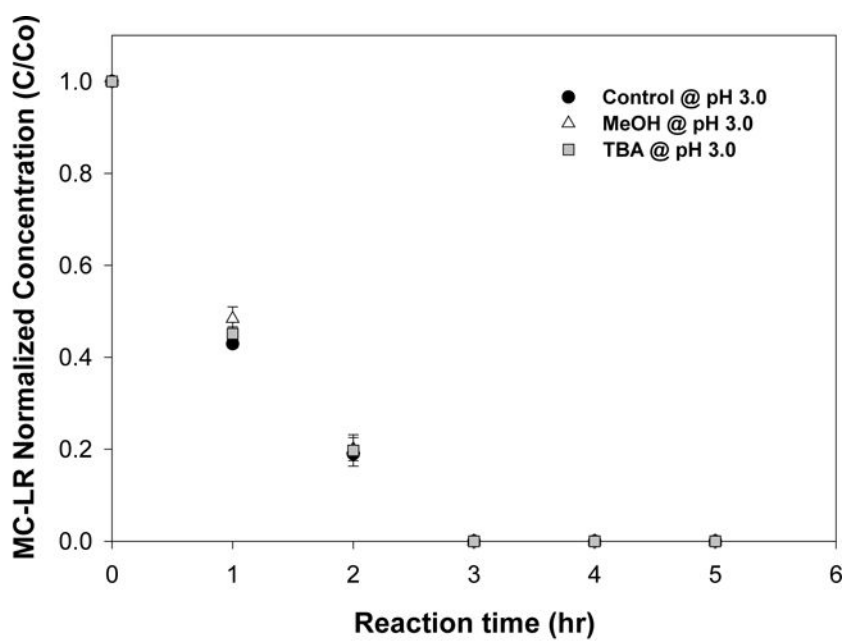


Figure 1. Photocatalytic degradation of MC-LR with NF-TiO₂ in the absence and presence of methanol and tert-butyl alcohol as $\cdot\text{OH}$ scavengers under visible light at a) pH 3.0 b) pH 5.7.

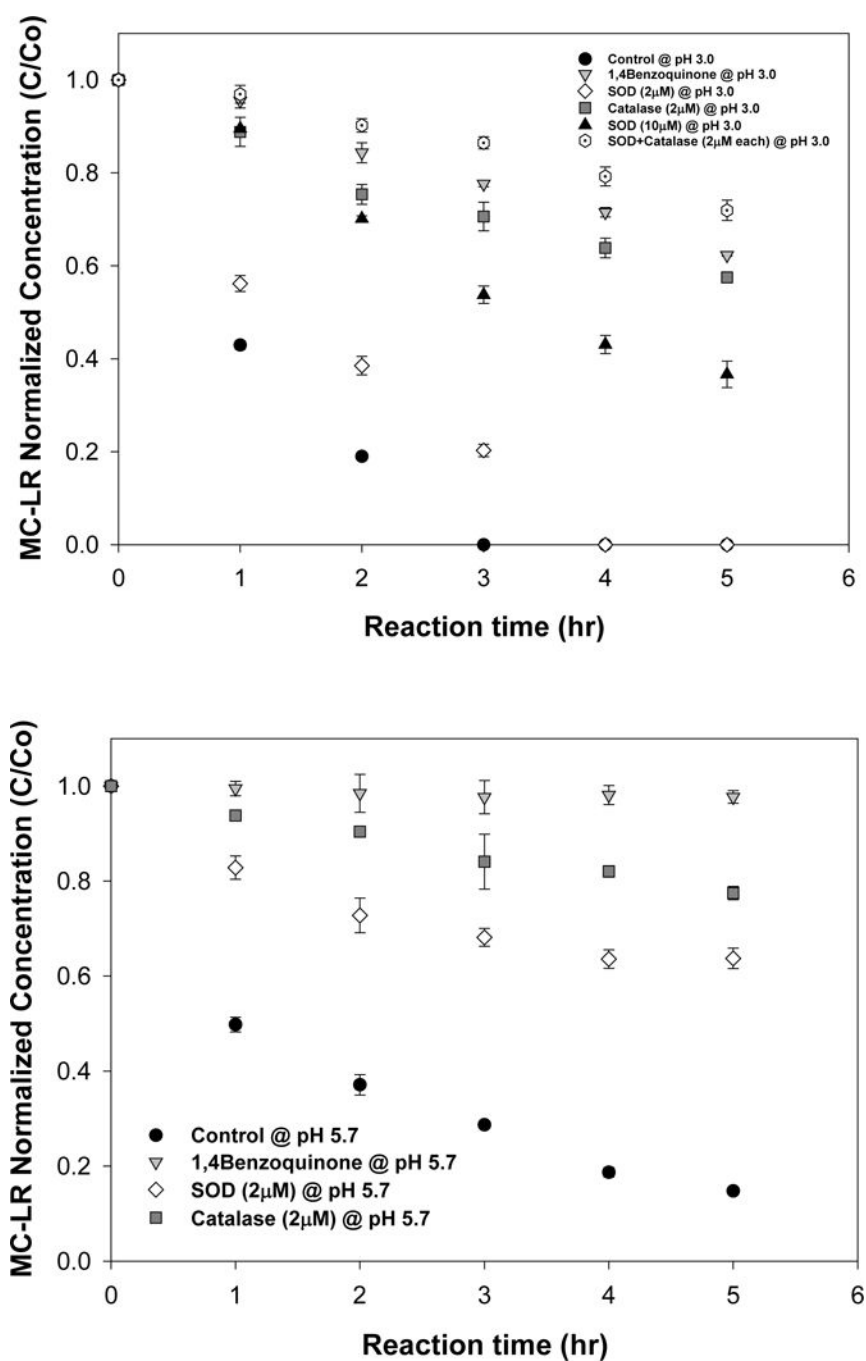


Figure 2. Photocatalytic degradation of MC-LR with NF-TiO₂ in the absence and presence of SOD and 1,4-benzoquinone as O₂^{•-} scavenger and catalase as H₂O₂ scavenger under visible light at a) pH 3.0 and b) pH 5.7.

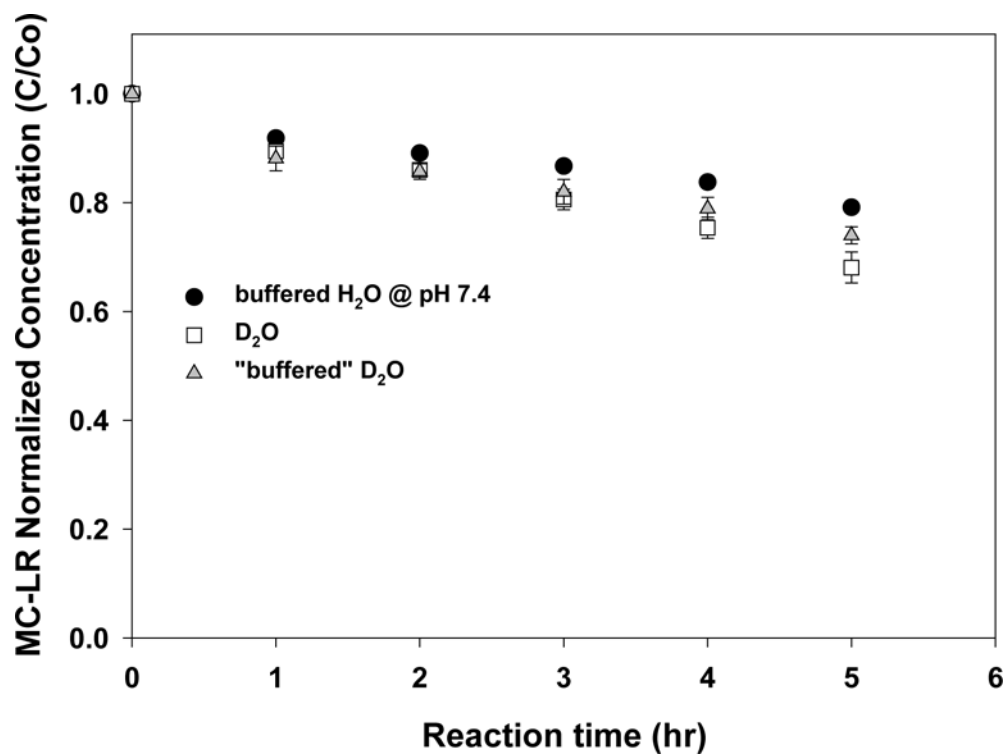


Figure 3. Photocatalytic degradation of MC-LR with buffered H₂O and D₂O with NF-TiO₂ under visible light.

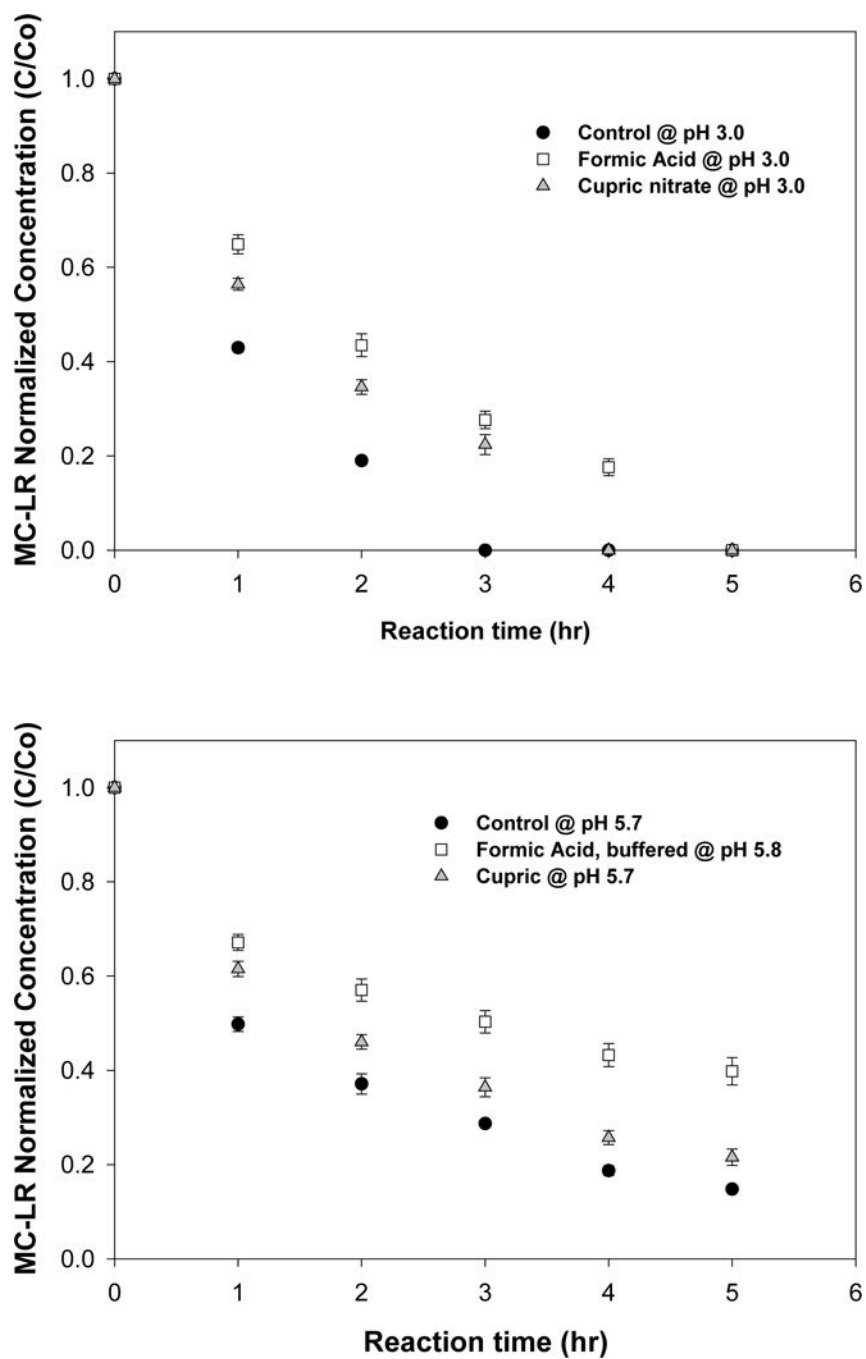


Figure 4. Effect of Cu(NO₃)₂ and formic acid addition as e⁻ and h⁺ scavenger, respectively, in NF-TiO₂ photocatalysis of MC-LR under visible light at a) pH 3.0 and b) pH 5.7.

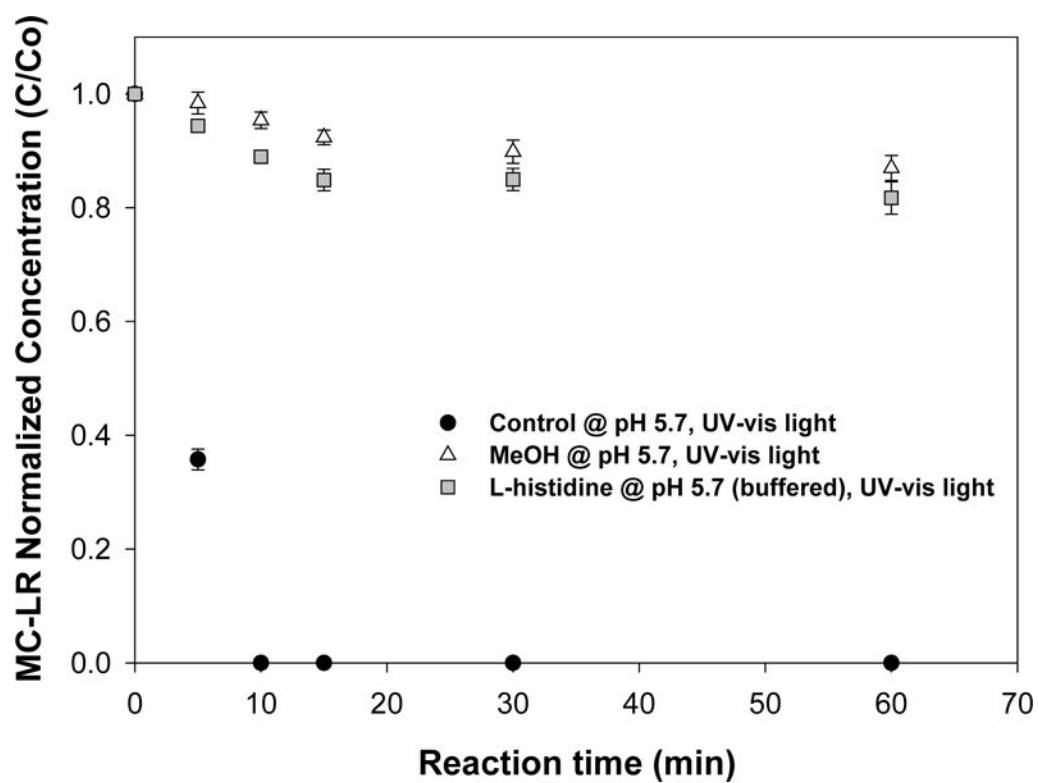
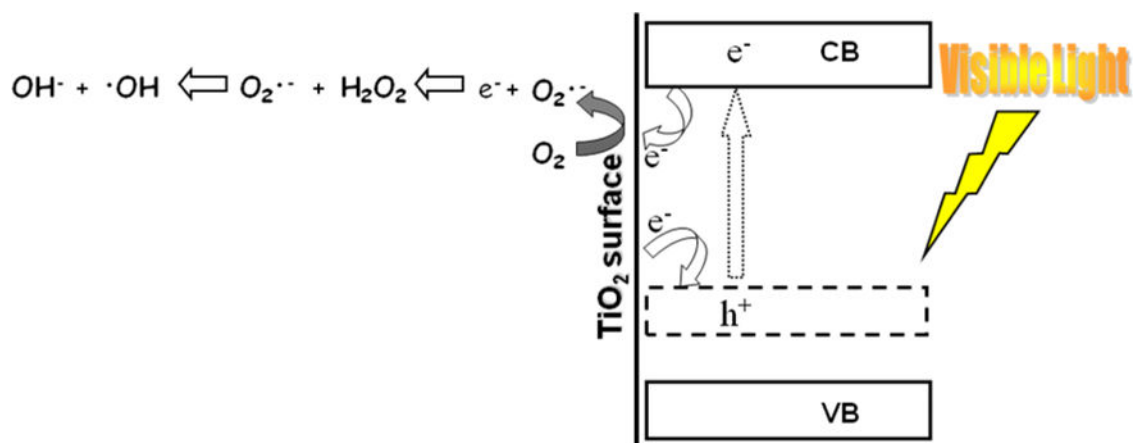


Figure 5. Photocatalytic degradation of MC-LR with NF-TiO₂ under UV+vis light and the scavenger effect of [•]OH with methanol and L-histidine.

**Scheme 1.**

Proposed mechanism of NF-TiO₂ photoactivation under visible light.

Table 1

List of compounds selected as scavengers for $\cdot\text{OH}$, $\text{O}_2^{\cdot-}$, $^1\text{O}_2$, H_2O_2 , e^- , and h^+ .

Compound	Scavenger type
Formic acid	h^+ scavenger
Cupric Nitrate	e^- scavenger
Methanol	$\cdot\text{OH}$
Tertbutanol	$\cdot\text{OH}$
D_2O^*	$^1\text{O}_2$
1,4-benzoquinone	$\text{O}_2^{\cdot-}$
Superoxide dismutase	$\text{O}_2^{\cdot-}$
Catalase	H_2O_2

* lifetime of singlet oxygen is 55 μsec in D_2O compared to 4.2 μsec in H_2O [34]